

The impact of gaseous degradation on the equilibrium state of gas/particle partitioning of semi-volatile organic compounds

Fu-Jie Zhu^{a,b,c}, Zi-Feng Zhang^{a,b}, Li-Yan Liu^{a,b}, Pu-Fei Yang^{a,b}, Peng-Tuan Hu^{a,d},
Geng-Bo Ren^c, Meng Qin^{a,b}, Wan-Li Ma^{a,b,*}

^a International Joint Research Center for Persistent Toxic Substances (IJRC-PTS), State Key Laboratory of Urban Water Resource and Environment, Harbin Institute of Technology, Harbin 150090, China

^b Heilongjiang Provincial Key Laboratory of Polar Environment and Ecosystem (HPKL-PEE), Harbin 150090, China

^c School of Energy and Environmental Engineering, Hebei University of Technology, Tianjin 300401, China

^d School of Environment, Key Laboratory for Yellow River and Huai River Water Environment and Pollution Control, Ministry of Education, Henan Normal University, Xinxiang 453007, China

*Corresponding author. International Joint Research Center for Persistent Toxic Substances (IJRC-PTS), State Key Laboratory of Urban Water Resource and Environment, Harbin Institute of Technology, 73 Huanghe Road, Nangang District, Harbin 150090, Heilongjiang, China.
Email address: mawanli002@163.com

Contents

Tables

Table S1. Information of 49 Me-PAHs	3
Table S2. Values and the calculation parameters for <i>A</i> and <i>B</i> of several Me-PAHs.....	6
Table S3. Calculation parameters for $\log K_{OA}$ (25°C) and ΔH_{OA} (kJ/mol).....	8
Table S4. The geometric mean values of the N/D ratios for different phases Me-PAHs in different seasons	9
Table S5. Gaseous degradation rate (h^{-1}) (hydroxyl radicals reaction) of Me-Naps and U-PAHs calculated using half-lives from EPI suite	11

Figures

Fig. S1. Chromatographic separation of 49 Me-PAHs in standard solutions (100 ng/mL)	13
Fig. S2. Comparison of the values of N/D ratios for individual Me-PAHs between particle phase and gas phase	14
Fig. S3. Comparison the regression lines of $\log K_p'$ vs. $\log K_{OA}$ of total Me-PAHs from daytime and nighttime	15
Fig. S4. Comparison of the regression lines of $\log K_p'$ against $\log K_{OA}$ between daytime and nighttime for part of individual Me-PAHs	16
Fig. S5. The fluxes related to the gas and particle phase in the six-compartment model....	17

Table S1. Information of 49 Me-PAHs

Compounds	Abbreviations	Categories	Rings	Quantitative ions	Qualitative ions	Retention time (min)	IDLs ^a (ng)	DR ^b
2-Methylnaphthalene	2-MeNap	Me	2	142	141	6.858	0.0384	84%
1-Methylnaphthalene	1-MeNap	Me	2	142	141	6.991	0.0505	85%
<u>2,6&2,7-Dimethylnaphthalene</u>	2,6&2,7-DMeNap	Me	2	156	141	7.710	0.0154	46%
1,3-Dimethylnaphthalene	1,3-DMeNap	Me	2	156	141	7.844	0.0904	70%
1,6-Dimethylnaphthalene	1,6-DMeNap	Me	2	156	141	7.886	0.0857	73%
<u>1,4&1,5-Dimethylnaphthalene</u>	1,4&1,5-DMeNap	Me	2	156	141	8.086	0.0467	74%
1,2-Dimethylnaphthalene	1,2-DMeNap	Me	2	156	141	8.220	0.138	68%
1,8-Dimethylnaphthalene	1,8-DMeNap	Me	2	156	141	8.462	0.126	-
2-Methylphenanthrene	2-MePhe	Me	3	192	191	17.476	0.310	96%
2-Methylantracene	2-MeAnt	Me	3	192	191	17.648	0.240	88%
1-Methylantracene	1-MeAnt	Me	3	192	191	17.812	0.207	-
1-Methylphenanthrene	1-MePhe	Me	3	192	191	17.855	0.239	98%
9-Methylantracene	9-MeAnt	Me	3	192	191	18.321	0.432	56%
3,6-Dimethylphenanthrene	3,6-DMePhe	Me	3	206	191	18.847	0.134	-
2,3-Dimethylantracene	2,3-DMeAnt	Me	3	206	191	19.606	0.201	-
9-Methyl-9-phenylfluorene	9-Me-9-PFlu	Me	4	241	256	20.015	0.0335	-
9,10-Dimethylantracene	9,10-DMeAnt	Me	3	206	191	20.155	0.245	-
2-Methylfluoranthene	2-MeFluo	Me	4	216	215	20.646	0.0636	97%
1-Methylpyrene	1-MePyr	Me	4	216	215	21.453	0.0620	97%
1-Methylbenzo[c]phenanthrene	1-MeBcP	Me	4	242	241	22.584	0.0570	92%
2-Methylbenzo[c]phenanthrene	2-MeBcP	Me	4	242	241	23.230	0.0275	84%

continued Table S1

Compounds	Abbreviations	Categories	Rings	Quantitative ions	Qualitative ions	Retention time (min)	IDLs ^a (ng)	DR ^b
3-Methylbenzo[c]phenanthrene	3-MeBcP	Me	4	242	241	23.623	0.0700	84%
5-Methylbenzo[c]phenanthrene	5-MeBcP	Me	4	242	241	23.800	0.0641	-
4-Methylbenzo[c]phenanthrene	4-MeBcP	Me	4	242	241	23.846	0.0673	-
<u>1&2-Methylbenz[a]anthracene</u>	1&2-MeBaA	Me	4	242	241	24.138	0.0367	74%
<u>7&9-Methylbenz[a]anthracene</u>	7&9-MeBaA	Me	4	242	241	24.254	0.0331	70%
<u>6&4-Methylbenz[a]anthracene</u>	6&4-MeBaA	Me	4	242	241	24.308	0.0313	62%
1,12-Dimethylbenzo[c]phenanthrene	1,12-DMeBcP	Me	4	256		24.469	0.0607	-
<u>5&6&4-Methylchrysene & 3&5-Methylbenz[a]anthracene</u>	5&6&4-MeChr&3&5-MeBaA	Me	4	242	241	24.500	0.0214	98%
10-Methylbenz[a]anthracene	10-MeBaA	Me	4	242	241	24.893	0.103	-
5,8-Dimethylbenzo[c]phenanthrene	5,8-DMeBcP	Me	4	256	239	25.270	0.0933	-
6,8-Dimethylbenz[a]anthracene	6,8-DMeBaA	Me	4	256	239	25.462	0.0908	-
3,9-Dimethylbenz[a]anthracene	3,9-DMeBaA	Me	4	256	239	25.578	0.108	50%
7,12-Dimethylbenz[a]anthracene	7,12-DMeBaA	Me	4	256	239	26.457	0.190	-
3-Methylcholanthrene	3-Me-Cho	Me	5	268	253	29.440	0.951	-
9-Methylbenzo[a]pyrene	9-MeBaP	Me	5	266	265	29.728	0.595	-
8-Methylbenzo[a]pyrene	8-MeBaP	Me	5	266	265	29.929	0.271	-
<u>7&10-Methylbenzo[a]pyrene</u>	7&10-MeBaP	Me	5	266	265	30.252	0.590	-
7,10-Dimethylbenzo[a]pyrene	7,10-DMeBaP	Me	5	280	131	33.153	0.505	-

Note: Underlined compounds represent that the instrumental method cannot achieve chromatographic separation for these compounds with same quantitative and qualitative ions

a, represents instrument detection limits

b, represents detection rate of all samples (include gaseous and particulate samples)

“-” represents the detection rate was below 30%

Table S2. Values and the calculation parameters for *A* and *B* of several Me-PAHs

Compounds	E ^a	S ^a	A ^a	B ^a	V ^a	L ^a	log <i>K</i> _{OA} (25°C) ^b	Δ <i>H</i> _{OA} (kJ/mol) ^b	<i>A</i> ^c	<i>B</i> ^c
2-MeNap	1.3	0.81	0	0.25	1.2263	5.617	5.51	56.43	-4.38	2948
1-MeNap	1.34	0.94	0	0.22	1.2263	5.802	5.73	57.16	-4.28	2986
2,6-DMeNap	1.35	0.82	0	0.25	1.3672	6.146	6.01	61.26	-4.72	3200
2,7-DMeNap	1.35	0.82	0	0.25	1.3672	6.147	6.01	61.27	-4.72	3201
1,3-DMeNap	1.39	0.92	0	0.2	1.3672	6.236	6.1	61.07	-4.60	3190
1,6-DMeNap	1.37	0.94	0	0.21	1.3672	6.347	6.23	62.11	-4.65	3244
1,4-DMeNap	1.4	0.91	0	0.2	1.3672	6.339	6.19	62.12	-4.69	3245
1,5-DMeNap	1.4	1.05	0	0.18	1.3672	6.545	6.45	63.08	-4.60	3295
1,2-DMeNap	1.43	0.97	0	0.25	1.3672	6.473	6.38	63.51	-4.75	3318
1,8-DMeNap	1.4	1.01	0	0.21	1.3672	6.653	6.55	64.64	-4.78	3377
2-MePhe	2.06	1.25	0	0.29	1.5953	8.307	8.16	79.55	-5.78	4155
2-MeAnt	2.29	1.3	0	0.31	1.5953	8.184	8.04	78.25	-5.67	4088
1-MeAnt	2.29	1.3	0	0.3	1.5953	8.332	8.17	79.59	-5.77	4158
1-MePhe	2.06	1.25	0	0.29	1.5953	8.408	8.26	80.53	-5.85	4207
9-MeAnt	2.25	1.27	0	0.3	1.5953	8.438	8.27	80.79	-5.88	4220
3,6-DMePhe	2.05	1.29	0	0.29	1.7362	8.7	8.56	82.89	-5.96	4330
9,10-DMeAnt	2.25	1.25	0	0.28	1.7362	9.283	9.04	88.67	-6.50	4632
1-MePyr	2.81	1.7	0	0.26	1.7255	9.541	9.4	88.28	-6.07	4611
1-MeBaA	2.99	1.7	0	0.35	1.9643	10.763	10.58	100.54	-7.03	5252
7-MeBaA	2.99	1.7	0	0.35	1.9643	11.096	10.89	103.76	-7.29	5420
4-MeBaA	2.99	1.7	0	0.35	1.9643	10.909	10.72	101.95	-7.14	5326
5-MeChr	3.03	1.73	0	0.36	1.9643	10.905	10.73	101.82	-7.11	5319

continued Table S2

Compounds	E ^a	S ^a	A ^a	B ^a	V ^a	L ^a	log K_{OA} (25°C) ^b	ΔH_{OA} (kJ/mol) ^b	A ^c	B ^c
6-MeChr	3.03	1.73	0	0.36	1.9643	10.934	10.76	102.1	-7.13	5333
4-MeChr	3.03	1.73	0	0.36	1.9643	10.937	10.76	102.13	-7.13	5335
7,12-DMeBaA	2.99	1.65	0	0.35	2.1052	11.753	11.48	110.19	-7.83	5756
3-MeCho	3.26	1.57	0	0.51	2.1375	12.482	12.19	119.14	-8.68	6223

Note:

a, Ulrich, N., Endo, S., Brown, T.N., Watanabe, N., Bronner, G., Abraham, M.H., Goss, K.-U., UFZ-LSER database v 3.2.1 [Internet], Leipzig, Germany, Helmholtz Centre for Environmental Research-UFZ. 2017 [accessed on 09.08.2022]. Available from <http://www.ufz.de/lserd>

b, log K_{OA} (25°C) and ΔH_{OA} (kJ/mol) were calculated using the parameters in **Table S1 and S2**.

c, B is calculated by the equation: $B = \Delta H_{OA} / (\ln(10) * 8.314)$, A is calculated by the equation: $A = \log K_{OA} (25^\circ\text{C}) - B / 298.15$

Table S3. Calculation parameters for $\log K_{OA}$ (25°C) and ΔH_{OA} (kJ/mol)

Parameters	e	s	a	b	v	l	constant	Equations	References
$\log K_{OA}$ (25°C)	-0.21	0.56	3.51	0.75		0.94	-0.15	Parameter = l * L + s * S + a * A + b * B + e * E + constant	[1]
ΔH_{OA} (kJ/mol)		-6.04	53.66	9.19	-1.57	9.66	6.67	Parameter = l * L + s * S + a * A + b * B + v * V + constant	[2]

References:

- [1] Abraham, M. H.; Smith, R. E.; Luchtefeld, R.; Boorem, A. J.; Luo, R. S.; Acree, W. E. J. *Pharma. Sci.* 2010, 99 (3), 1500-1627
- [2] Mintz, C.; Burton, K.; Ladlie, T.; Clark, M.; Acree Jr, W. E.; Abraham, M. H. *Thermochim. Acta* 2008, 470 (1-2), 67-76.

Table S4. The geometric mean values of the N/D ratios for different phases Me-PAHs in different seasons

	Total Phase			Particle Phase			Gas Phase		
	All season	Heating season	Non-heating season	All season	Heating season	Non-heating season	All season	Heating season	Non-heating season
2-MeNap	2.67	2.14	3.30	0.842	0.561	2.23	2.73	2.21	3.33
1-MeNap	3.16	2.22	4.41	0.819	0.493	2.47	3.25	2.30	4.51
2,6&2,7-DMeNap	2.19	2.02	7.30	0.347	0.347	-	2.37	2.19	7.30
1,3-DMeNap	2.97	2.01	4.27	0.588	0.499	3.03	3.03	2.11	4.27
1,6-DMeNap	2.76	1.93	3.85	0.604	0.528	1.18	2.83	2.03	3.87
1,4&1,5-DMeNap	2.67	1.88	3.72	0.501	0.429	3.28	2.73	1.96	3.72
1,2-DMeNap	2.45	1.75	3.35	0.557	0.557	-	2.49	1.82	3.35
2-MePhe	1.11	1.12	1.10	1.09	0.984	1.24	1.11	1.14	1.09
2-MeAnt	1.20	1.32	1.11	1.68	1.34	2.94	1.04	1.05	1.03
1-MePhe	1.15	1.12	1.18	1.08	0.975	1.22	1.15	1.14	1.17
9-MeAnt	2.07	2.49	1.38	2.04	2.04	-	1.89	2.78	1.28
2-MeFluo	1.36	1.23	1.50	1.61	1.24	2.05	1.05	0.68	1.46
1-MePyr	1.65	1.39	1.95	1.97	1.40	2.71	1.31	0.81	1.89
1-MeBcP	1.93	1.25	2.88	1.83	1.30	2.63	1.86	1.01	2.79
2-MeBcP	1.73	1.26	2.34	1.90	1.27	2.78	1.56	1.12	1.72
3-MeBcP	1.61	1.27	2.01	1.67	1.26	2.24	1.45	1.15	1.54
1&2-MeBaA	2.04	1.57	2.61	2.08	1.56	2.72	1.79	0.87	2.70
7&9-MeBaA	1.69	1.35	2.11	1.61	1.34	1.99	1.22	1.48	1.15
6&4-MeBaA	1.85	1.44	2.33	1.84	1.44	2.31	1.22	-	1.22

continued Table S4

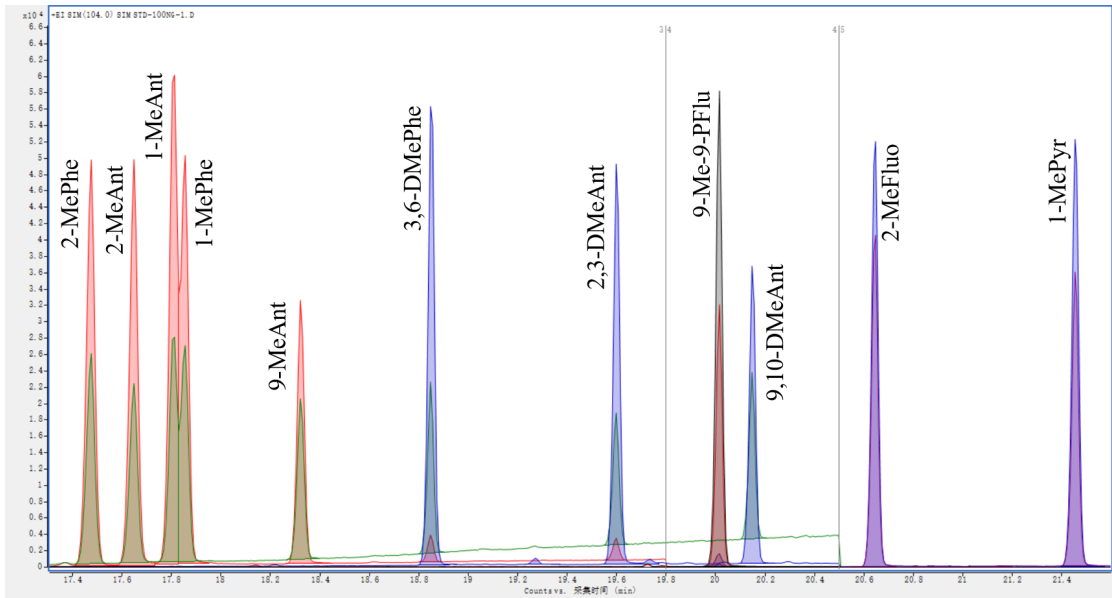
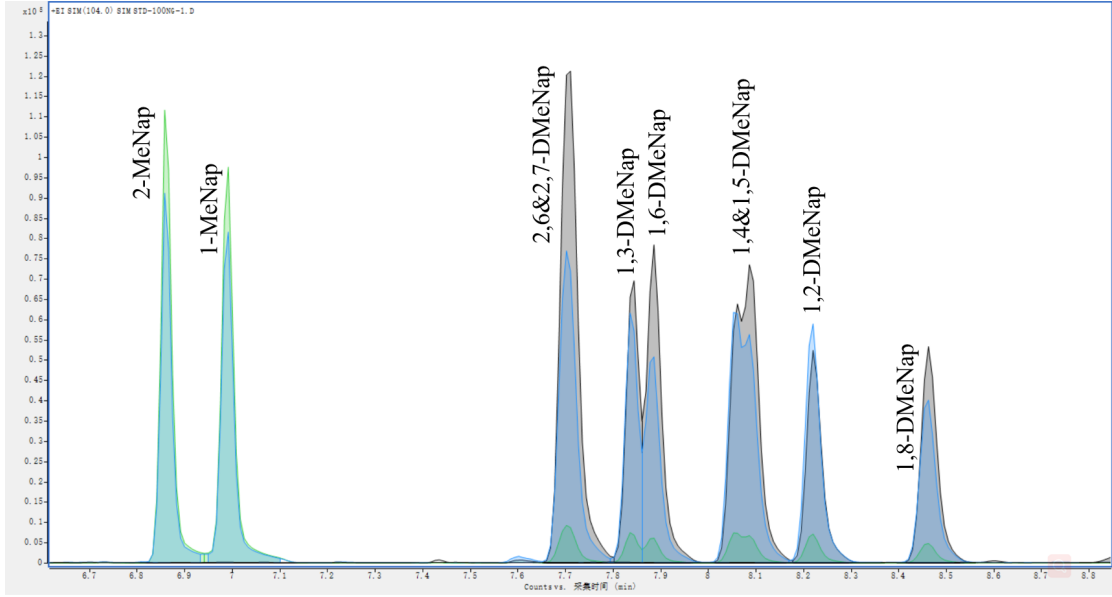
	Total Phase			Particle Phase			Gas Phase		
	All season	Heating season	Non-heating season	All season	Heating season	Non-heating season	All season	Heating season	Non-heating season
5&6&4-MeChr&3&5-MeBaA	1.90	1.46	2.42	2.01	1.46	2.77	1.31	1.17	1.46
3,9-DMeBaA	1.86	1.72	2.01	1.86	1.72	2.01	-	-	-
Number of significance	13	6	14	6	3	11	10	7	8

Note: The bold Numbers represent the mean concentrations of Me-PAHs in nighttime were significant different with that in daytime ($p < 0.05$).

Table S5. Gaseous degradation rate (h^{-1}) (hydroxyl radicals reaction) of Me-Naps and U-PAHs calculated using half-lives from EPI suite

PAHs	$k_{\text{deg_25}}$	$k_{\text{deg_min}}$	$k_{\text{deg_max}}$
2-MeNap	0.305	0.0787	0.417
1-MeNap	0.305	0.0787	0.417
2,6&2,7-DMeNap	0.375	0.0966	0.512
1,3-DMeNap	0.375	0.0966	0.512
1,6-DMeNap	0.375	0.0966	0.512
1,4&1,5-DMeNap	0.375	0.0966	0.512
1,2-DMeNap	0.375	0.0966	0.512
Acy	0.408	0.118	0.557
Ace	0.361	0.105	0.493
Flu	0.0478	0.0139	0.0653

Note: The gaseous degradation rate of PAHs can be calculated using the half-lives of PAHs: $k_{\text{degi}} = \ln(2)/t_{1/2}$.



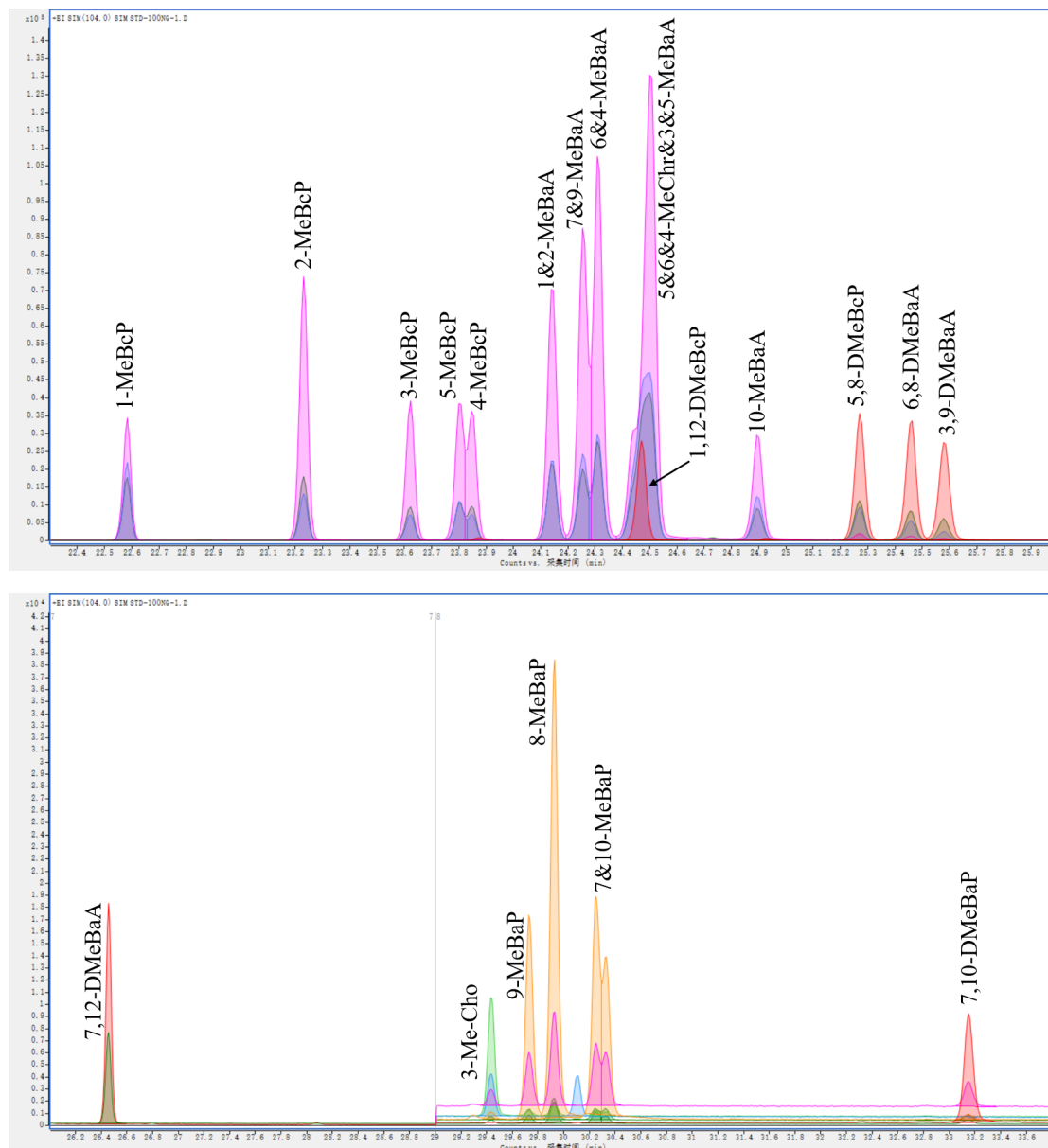


Fig. S1. Chromatographic separation of 49 Me-PAHs in standard solutions (100 ng/mL)

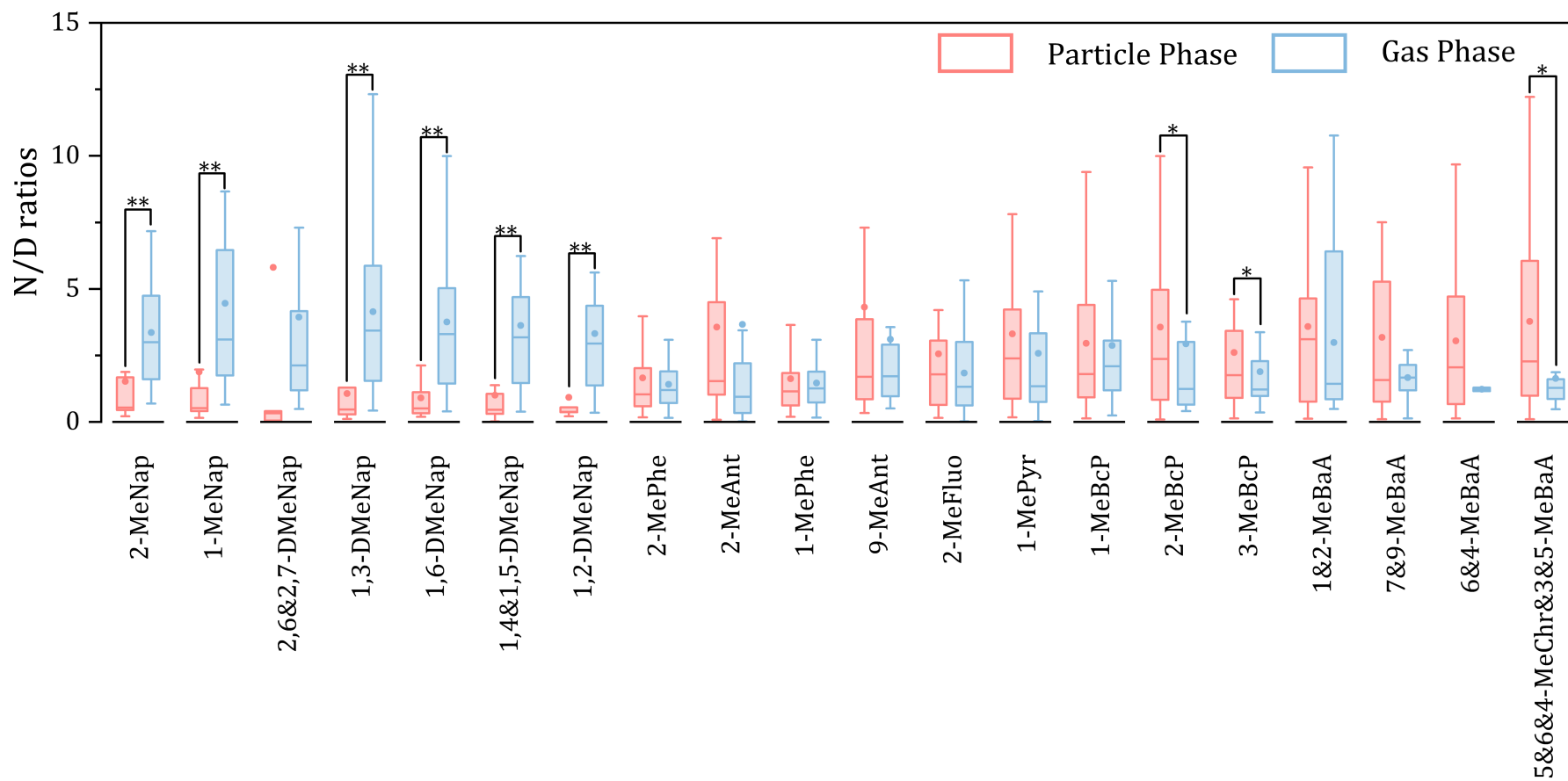


Fig. S2. Comparison of the values of N/D ratios for individual Me-PAHs between particle phase and gas phase

(Note: * and ** represent that the differences are significant at 0.05 and 0.01 level.)

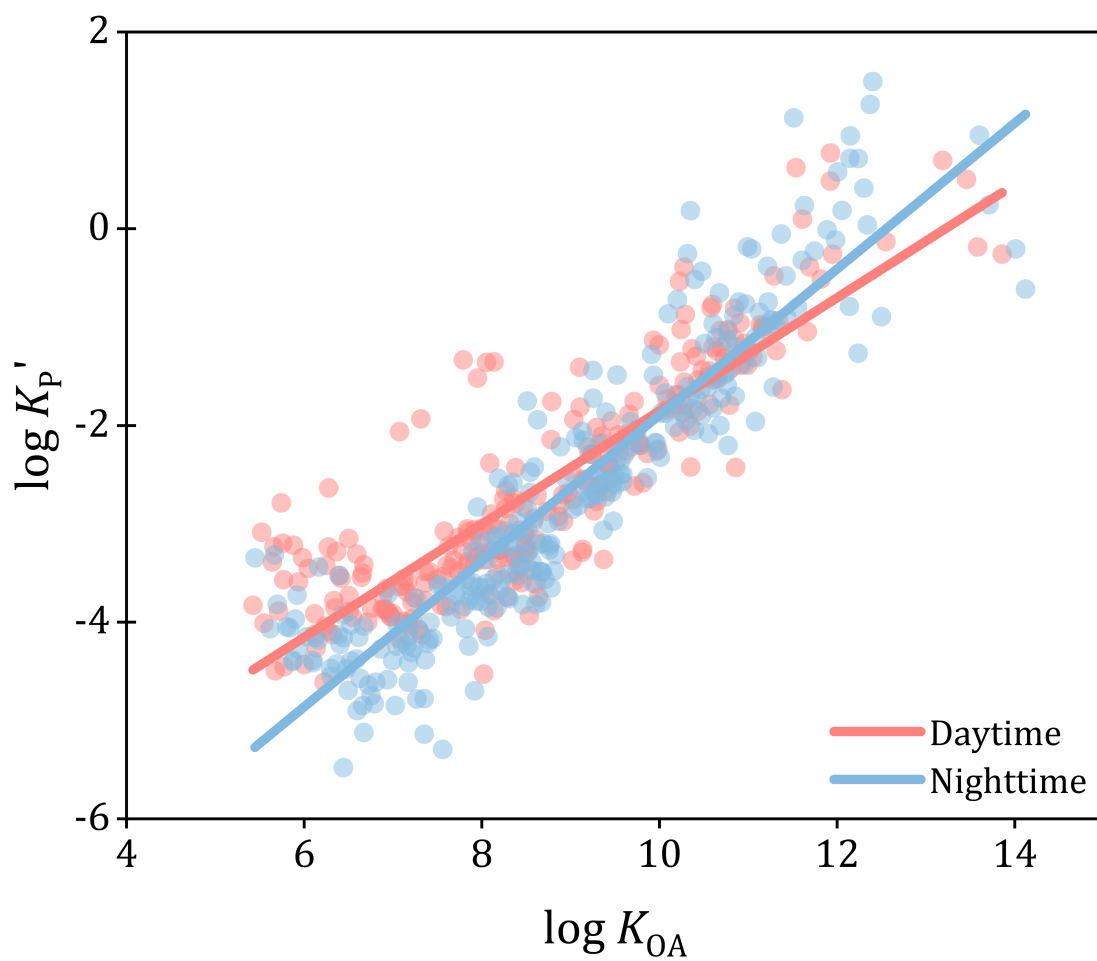


Fig. S3. Comparison the regression lines of $\log K_{P'}$ vs. $\log K_{OA}$ of total Me-PAHs from daytime and nighttime

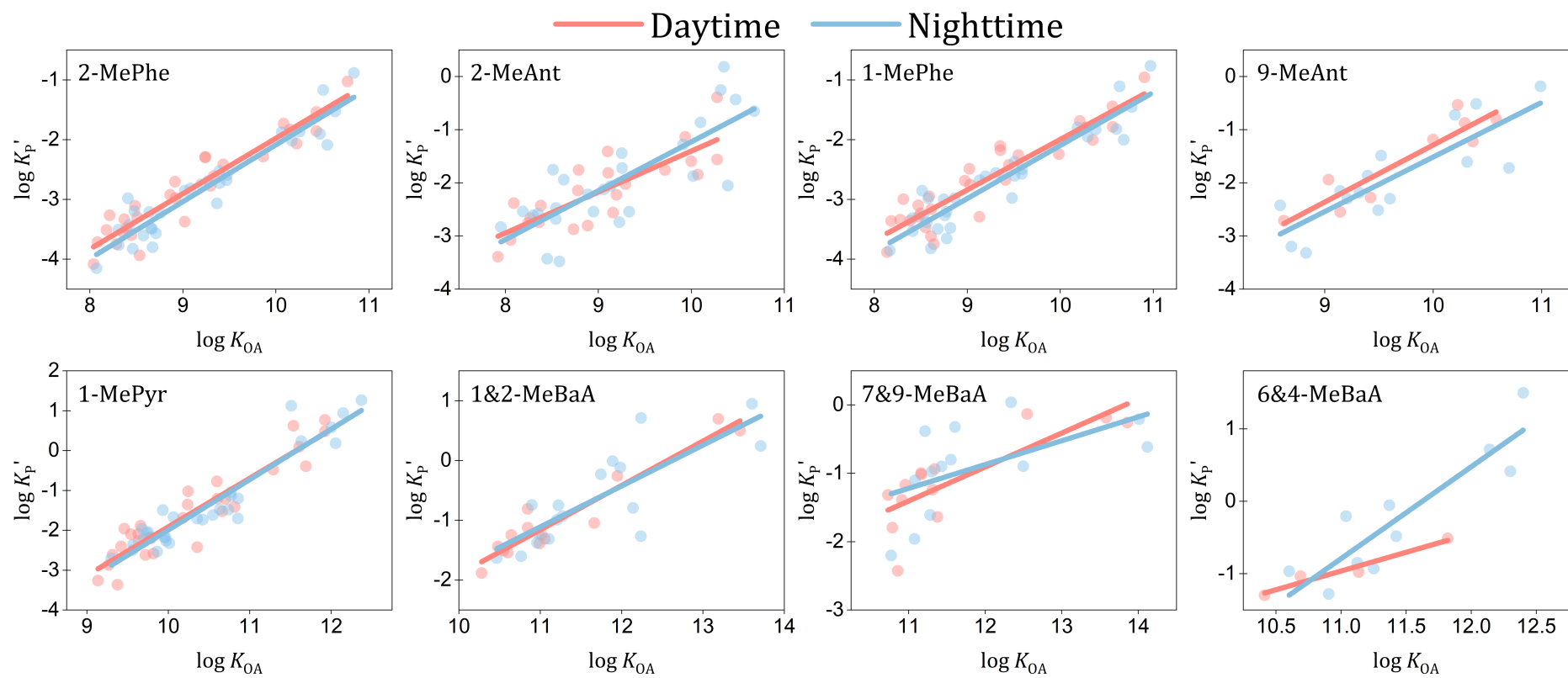


Fig. S4. Comparison of the regression lines of $\log K_{P'}$ against $\log K_{OA}$ between daytime and nighttime for part of individual Me-PAHs

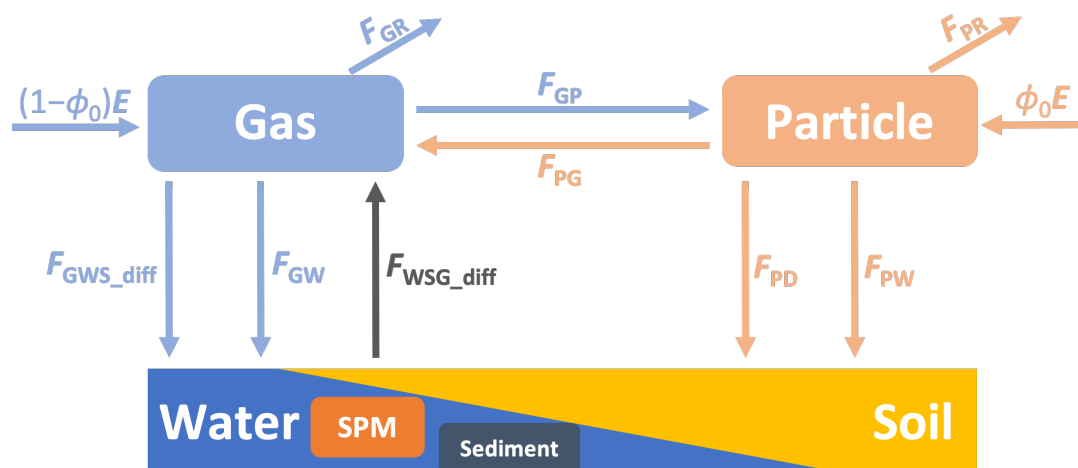


Fig. S5. The fluxes related to the gas and particle phase in the six-compartment model

(Note: F_{GR} : degradation flux of gas phase PAHs; F_{PR} : degradation flux of particle phase PAHs; F_{GP} : migration flux from gas phase to particle phase; F_{PG} : migration flux from particle phase to gas phase; F_{GWS_diff} : diffusion fluxes from gas phase to water and/or soil phases; F_{GW} : wet deposition flux of gas phase PAHs to water and/or soil phase; F_{WSG_diff} : diffusion fluxes from soil and/or water phases to gas phase; F_{PD} : dry deposition flux of particle phase PAHs to SPM and/or soil phase; F_{PW} : wet deposition flux of particle phase PAHs to SPM and/or soil phase; $(1-\phi_0)E$: emission flux of gas phase PAHs; $\phi_0 E$: emission flux of particle phase PAHs.)

The Figure was cited from the reference: Zhu Fu-Jie, Hu Peng-Tuan, Ma Wan-Li. A new steady-state gas-particle partitioning model of polycyclic aromatic hydrocarbons: implication for the influence of the particulate proportion in emissions. *Atmospheric Chemistry and Physics* 2023; 8583–8590.